Am J Physiol Renal Physiol 305: F1139–F1148, 2013.
First published August 14, 2013; doi:10.1152/ajprenal.00259.2013.

Dietary salt intake modulates differential splicing of the Na-K-2Cl cotransporter NKCC2

Ina Maria Schieβl,[1] Agnes Rosenauer,[1] Veronika Kattler,[1] Will W. Minuth,[2] Mona Oppermann,[3] and Hayo Castrop[1]

[1]*Institute of Physiology University of Regensburg, Regensburg, Germany;* [2]*Institute of Molecular and Cellular Anatomy, University of Regensburg, Regensburg, Germany; and* [3]*Children's Hospital, University Medical Center, Regensburg, Germany*

Submitted 7 May 2013; accepted in final form 12 August 2013

Schieβl IM, Rosenauer A, Kattler V, Minuth WW, Oppermann M, Castrop H. Dietary salt intake modulates differential splicing of the Na-K-2Cl cotransporter NKCC2. *Am J Physiol Renal Physiol* 305: F1139–F1148, 2013. First published August 14, 2013; doi:10.1152/ajprenal.00259.2013.—Both sodium reabsorption in the thick ascending limb of the loop of Henle (TAL) and macula densa salt sensing crucially depend on the function of the Na/K/2Cl cotransporter NKCC2. The NKCC2 gene gives rise to at least three different full-length NKCC2 isoforms derived from differential splicing. In the present study, we addressed the influence of dietary salt intake on the differential splicing of NKCC2. Mice were subjected to diets with low-salt, standard salt, and high-salt content for 7 days, and NKCC2 isoform mRNA abundance was determined. With decreasing salt intake, we found a reduced abundance of the low-affinity isoform NKCC2A and an increase in the high-affinity isoform NKCC2B in the renal cortex and the outer stripe of the outer medulla. This shift from NKCC2A to NKCC2B during a low-salt diet could be mimicked by furosemide in vivo and in cultured kidney slices. Furthermore, the changes in NKCC2 isoform abundance during a salt-restricted diet were partly mediated by the actions of angiotensin II on AT_1 receptors, as determined using chronic angiotensin II infusion. In contrast to changes in oral salt intake, water restriction (48 h) and water loading (8% sucrose solution) increased and suppressed the expression of all NKCC2 isoforms, without changing the distribution pattern of the single isoforms. In summary, the differential splicing of NKCC2 pre-mRNA is modulated by dietary salt intake, which may be mediated by changes in intracellular ion composition. Differential splicing of NKCC2 appears to contribute to the adaptive capacity of the kidney to cope with changes in reabsorptive needs.

differential spacing; NKCC2; salt transport

THE THICK ASCENDING LIMB OF the loop of Henle (TAL) contributes to 25–30% of total renal Na^+ reabsorption. Apical Na uptake in cells of the TAL is primarily mediated by the bumetanide-sensitive Na-K-2Cl cotransporter NKCC2 (5). In addition to its function in TAL salt retrieval, the NKCC2-dependent transport activity of macula densa cells constitutes the initial step in the tubulovascular signaling pathways between the TAL in the juxtaglomerular region and the afferent arteriole (20, 33). By detecting changes in luminal NaCl concentration, macula densa cells modulate the tone of the afferent arteriole and subsequently control the single-nephron glomerular filtration rate. This negative feedback loop is known as tubuloglomerular feedback (TGF; Ref. 38). Macula densa cells also control the secretion of renin from granular cells of the afferent arteriole (4).

NKCC2 is encoded by the gene *Slc12a1* (8, 16). In humans and all other examined mammalian species, differential splicing of *Slc12a1* gives rise to at least three different full-length isoforms of NKCC2, known as NKCC2B, NKCC2A, and NKCC2F (3, 16, 28, 40). During the splicing process, the exon 3 is linked to the exon 4B or 4A or 4F followed by the common exon 5. Thus the NKCC2 isoforms differ in the variable exon 4, which encodes for 32 amino acids of the second transmembrane domain and parts of the adjacent intracellular loop (28). This part of the cotransporter has been shown to be crucial to Cl transport and loop diuretic binding (12).

The NKCC2 isoforms differ in their localization along the TAL and in their transport characteristics. In rodents, NKCC2F is predominantly expressed in the medullary TAL, and NKCC2A is expressed in the outer stripe of the outer medulla and in the cortical portions of the TAL. The latter NKCC2A expression overlaps with NKCC2B, which is predominantly expressed in the cortical TAL (26, 27, 42). In the macula densa, a parallel expression of NKCC2B and NKCC2A has been shown for mouse kidney (26, 27). The transport characteristics of the NKCC2 isoforms were addressed in several in vitro studies, indicating that the NKCC2F isoform has the lowest affinity for Cl, which is the transport-limiting ion. NKCC2A exerts a markedly higher Cl affinity than does NKCC2F; the NKCC2B has the highest Cl affinity but the lowest transport capacity (10, 29). These in vitro findings were further confirmed by in vivo micropuncture studies using mice with targeted disruption of NKCC2B and NKCC2A (26, 27).

In this study, we investigated the regulation of the differential splicing of NKCC2 in mice during changes in oral salt intake. Considering the differential expression patterns and transport characteristics of the NKCC2 isoforms, we hypothesized that the differential splicing of NKCC2 may be modulated to cope with changes in renal reabsorptive needs. Furthermore, we postulated that changes in the NKCC2 isoform expression in the macula densa may be involved in adaptations of the TGF, known as TGF resetting, in response to chronically altered tubular Cl concentrations (36, 37).

We found that differential NKCC2 splicing was modulated during changes in dietary salt intake such that salt restriction enhanced the expression of the high-affinity NKCC2B isoform and concomitantly reduced the levels of the lower-affinity A isoform. This regulation of the splicing process was partially dependent on the NKCC2 transport activity. The resulting changes in the specific NKCC2 isoform abundance may con-

Address for reprint requests and other correspondence: H. Castrop, Institute of Physiology, Univ. of Regensburg, Universitätsstr. 31, 93040 Regensburg, Germany (e-mail: hayo@castrop.com).

tribute to the overall adaptations of renal Na^+ homoeostasis and to the resetting of the operating point of the TGF.

METHODS

Animal Experiments

All experiments were performed in male 8- to 10-wk-old C57BL/6 mice. Animal care and experimentation were approved by local authorities (Regierung der Oberpfalz) and carried out in accordance with National Institutes of Health principles as outlined in their *Guide for the Care and Use of Laboratory Animals.*

Experimental Protocols

Changes in oral salt intake. Groups of six mice each received a low-salt diet [0.02% NaCl (wt/wt)], standard chow [0.4% NaCl (wt/wt)], or high-salt diet [4% NaCl (wt/wt)] for 7 days ($n = 6$). Experimental chow was purchased from Ssniff Spezialdiäten (Soest, Germany).

Furosemide infusion. Furosemide was applied by osmotic minipumps (model 1002; Alzet; 10 $mg \cdot kg^{-1} \cdot day^{-1}$) for 7 days. In a control group, the osmotic minipumps were filled with vehicle ($n = 6$ for each group). Pumps were implanted subcutaneously under sevoflurane anesthesia. The mice had free access to one bottle with tap water and one bottle containing a 1% NaCl solution.

Chronic infusion of angiotensin II. Mice were infused with angiotensin II for 7 days via osmotic minipumps. Minipumps were loaded with angiotensin II dissolved in 300 mM NaCl and 1 mM acetic acid (2 $mg \cdot kg^{-1} \cdot day^{-1}$ angiotensin II; Sigma-Aldrich). Pumps were implanted subcutaneously while the animals were under sevoflurane anesthesia ($n = 10$). A control group received osmotic minipumps filled with vehicle ($n = 10$). The function of the osmotic minipump was controlled by the determination of arterial blood pressure using tail-cuff manometry.

Angiotensin II receptor antagonism. Mice received the AT_1 receptor antagonist losartan (Sigma-Aldrich) dissolved in their drinking water for 7 days (30 $mg \cdot kg^{-1} \cdot day^{-1}$; $n = 6$). To block the AT_2 receptor, mice received PD123319 (10 $mg \cdot kg^{-1} \cdot day^{-1}$) in the drinking water (7 days). A control group had free access to tap water ($n = 6$).

Low-salt diet. The low-salt diet [0.02% NaCl (wt/wt)] was given in combination with the AT_1 receptor antagonist losartan (Sigma-Aldrich) dissolved in the drinking water for 7 days (30 $mg \cdot kg^{-1} \cdot day^{-1}$; $n = 6$).

Water restriction. Mice were kept for 48 h without access to water. A control group had free access to tap water ($n = 6$ each).

Water loading. Mice had access to tap water and a bottle with 8% sucrose solution ($n = 6$).

1-Desamino-8-D-arginine-vasopressin infusion. Mice were infused with 1-desamino-8-D-arginine-vasopressin (DDAVP; 2 $\mu g \cdot kg^{-1} \cdot day^{-1}$; Sigma) for 7 days via osmotic minipumps ($n = 6$).

RNA Isolation and Quantitative RT-PCR

To localize NKCC2 isoform expression to specific zones of the kidney, mouse kidney specimens were microdissected and divided into the cortex (CO), outer medulla outer stripe (OMOS), outer medulla inner stripe (OMIS), and inner medulla (IM). Complementary DNA (cDNA) was obtained by reverse transcription (M-MLV-RT; Invitrogen), and real-time PCR was performed for NKCC2 isoforms, β-actin, and GAPDH using a Light-Cycler system (Roche, Mannheim, Germany). NKCC2 isoform mRNA expression data were normalized to β-actin or GAPDH mRNA expression. The following isoform-specific oligonucleotide primers were used: 5′-gcctctcctggattgtaggagaa-3′ (common sense primer located in exon 3), 5′-cccagtgatagaggttaccatggt-3′ (antisense, NKCC2A), 5′-gacaaacctgtgatggctgtca-3′ (antisense, NKCC2B), and 5′-acaactacgctcaggccaatg-3′ (antisense, NKCC2F). To detect all isoforms (total NKCC2 expression), the common sense primer in exon 3 was combined with a common antisense primer in exon 5, located downstream of the variable exons 4B, 4A, and 4F (5′-ctaagctccgggaaatcaggta-3′).

Western Blotting

Western blotting for NKCC2, pNKCC2, and GAPDH was performed according to standard protocols using a membrane fraction obtained by differential centrifugation steps of whole kidney protein extracts. Twenty micrograms of the protein extract were loaded on SDS gels for the determinations of the NKCC2 and pNKCC2 abundance; 2 μg were loaded for GAPDH. Anti NKCC2 and pNKCC2 antibodies were a gift from Dr. Bachmann (Charite, Berlin; Ref. 22). The anti-GAPDH antibody was from Abnova (Walnut, CA). Secondary antibodies were horseradish peroxidase-conjugated, and X-ray films were evaluated densitometrically after chemiluminescence exposure (Bio1d, Vilber Lourmat, France).

Blood Pressure Determination

Systolic blood pressure was measured by tailcuff manometry, as described previously (26).

Determination of Urine Osmolarity

Urine osmolarities under ambient conditions were determined in spot urine samples of conscious mice by the freezing point depression method.

Perfusion Culture of Kidney Slices

Tissue culture was performed as described in detail recently (23, 35). In brief, kidneys were harvested and cut with a tissue chopper. Kidney slices (250 μm) were positioned between two layers of polyester fleece and transferred to a perfusion chamber (Minucells, Bad Abbach, Germany). The flow rate of the culture medium (IMDM; GIBCO) was adjusted to 2 ml/h and the following drugs were added for 48 h: angiotensin II (10 nM), losartan (100 nM), PD 123319 (100 nM), and furosemide (10 μM).

Statistics

Data are expressed as means and SE. Statistical comparisons were made by Student's *t*-test or by ANOVA with Bonferroni post hoc test when necessary.

RESULTS

Expression of NKCC2 Isoforms During Modulation of Oral Salt Intake

No specific antibodies are available that can distinguish between NKCC2 isoforms. This problem is related to the high homology of the amino acid sequences (32 aa) encoded by the variable exon 4 of the NKCC2 mRNA (Fig. 1). When NKCC2B is taken as a reference, NKCC2A and NKCC2F share 25 and 24 out of 32 amino acids encoded by the variable exon 4; with a total length of 1,095 amino acids for each NKCC2 isoform, these differences in the amino acid sequences result in an overall homology of 99.4 and 99.3% for NKCC2A and NKCC2F, respectively, compared with NKCC2B (Fig. 1).

Therefore, NKCC2 isoform expression was determined by quantitative RT-PCR using isoform-specific primers. This approach also ensured that no postsplicing events, such as modulation of translation efficiency, would mask changes in the splicing process. For a standard diet, NKCC2F was the dominant isoform in the OMIS with a declining gradient of expression towards the cortex. NKCC2A was mostly found in the

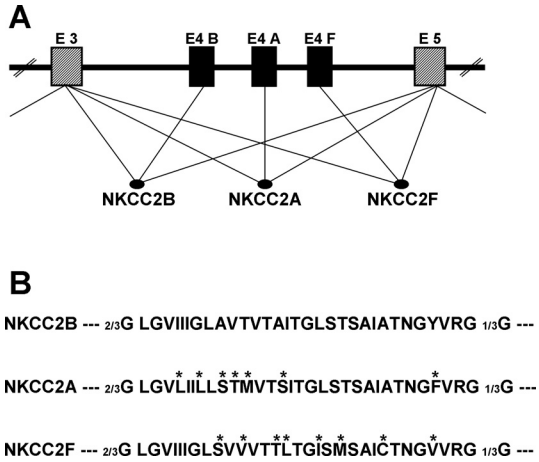

Fig. 1. *A*: schematic drawing of the Slc12a1 gene of the mouse showing the splicing process between the exon 3, the variable exons 4B, 4A, and 4F, and exon 5. *B*: alignment of the 32 amino acid sequence encoded by the variable exon 4. *Sequence differences compared with Na-K-2Cl cotransporter NKCC2B. The reading frame of the NKCC2 mRNA overlaps between exon 3/4 and 4/5. The total length of the NKCC2 protein is 1,095 amino acids.

OMOS and the cortex, where it overlapped with NKCC2B (Fig. 2). A reduction of oral salt intake (low-salt diet vs. standard diet vs. high-salt diet) slightly increased the expression of NKCC2F in the OMIS and OMOS. More noticeably, for a low-salt diet, the expression pattern of the NKCC2 isoforms shifted from NKCC2A to NKCC2B in the OMOS, and this shift was also observed in the cortex. Thus during a low-salt diet, the NKCC2A mRNA was reduced by 51 ± 5 and 45 ± 3% in the cortex and OMOS, respectively, and NKCC2B was increased by 105 ± 20 and 122 ± 10%, respectively (Fig. 2). These changes in the isoform expression levels resulted in an overall increase in NKCC2 mRNA abundance when the oral salt intake was reduced (Fig. 2).

NKCC2 protein and phospho-NKCC2 protein were determined after modulation of oral salt intake to asses how the changes in the single NKCC2 mRNA isoform expression levels would translate into net NKCC2 protein abundance. As shown in Fig. 3*A*, total NKCC2 protein abundance in whole kidneys during changes in dietary salt intake did not change significantly. The abundance of pNKCC2, normalized to the GAPDH abundance, however, increased during salt restriction averaging 2.57 ± 0.18, 1.73 ± 0.19, and 1.30 ± 0.23 rU for a low-salt diet, control diet, and high-salt diet, respectively (n = 4; $P < 0.05$ for low salt vs. control).

Influence of NKCC2 Transport Activity on NKCC2 Differential Splicing

Variation in oral salt intake may influence NKCC2 differential splicing by altering TAL transport activity. Therefore, we next determined the influence of inhibited NKCC2 transport on the splicing process. For this purpose, furosemide was applied via osmotic minipumps for 7 days. The urine osmolarity decreased from 1,625 ± 188 at baseline to 355 ± 100 mosmol/kgH_2O during furosemide treatment ($P < 0.01$; Table 1). As shown in Fig. 4, the total NKCC2 expression after furosemide infusion was unaltered in the cortex but reduced in the OMOS and OMIS, resulting in a slight reduction of the NKCC2 expression for the total kidney. The unchanged total NKCC2 expression in the cortex was accompanied by a marked shift of the expression levels of single NKCC2 isoforms, similar to what was seen after a salt-restricted diet (Fig. 4). Thus the NKCC2A expression was reduced by 70 ± 8% during furosemide treatment (n = 6; $P < 0.05$ vs. vehicle), whereas the NKCC2B mRNA abundance was increased by 64 ± 9% (n = 6; $P < 0.05$ vs. vehicle). There was a slight reduction of NKCC2F expression in the cortex after furosemide; however, the absolute cortical NKCC2F levels were very low (Fig. 4). A similar shift from NKCC2A to NKCC2B expression was also detected in the OMOS. The changes in the NKCC2B and NKCC2A abundance during furosemide treatment were paralleled by reduced NKCC2F levels in the OMOS and OMIS when compared with those in vehicle-infused mice (−45 and −27%, $P < 0.05$, respectively).

Influence of Angiotensin II on NKCC2 Differential Splicing

The previously mentioned conditions, such as modulation of oral salt intake, are accompanied by changes in the activity of

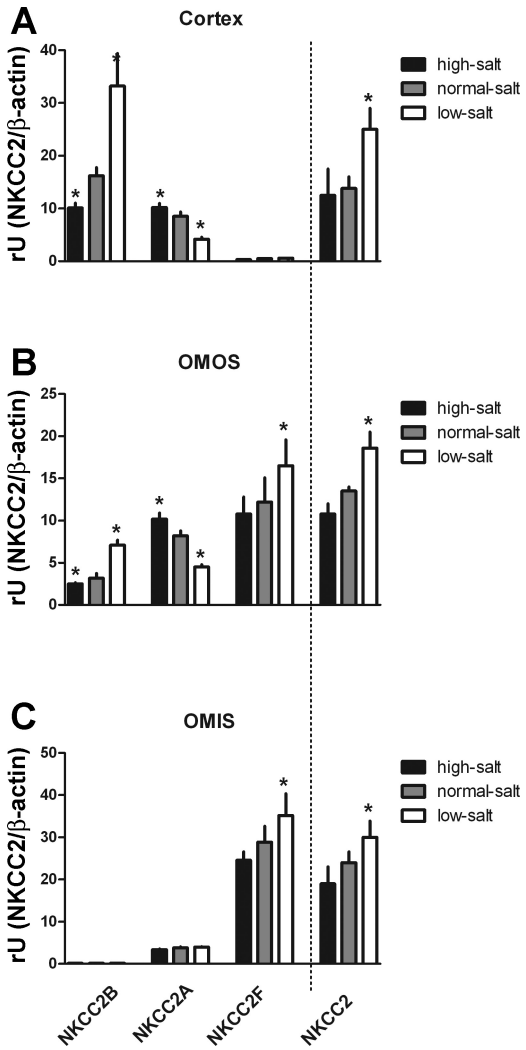

Fig. 2. Dietary salt intake modulates NKCC2 differential splicing. NKCC2 isoform expression in mice after 7 days on a high-salt [4% NaCl (wt/wt)], standard [0.4% NaCl (wt/wt)], and a low-salt diet [0.02% NaCl (wt/wt)], determined by quantitative RT-PCR in the renal cortex (*A*), outer medulla outer stripe (OMOS; *B*), and outer medulla inner stripe (OMIS; *C*). *$P < 0.05$ vs. control diet.

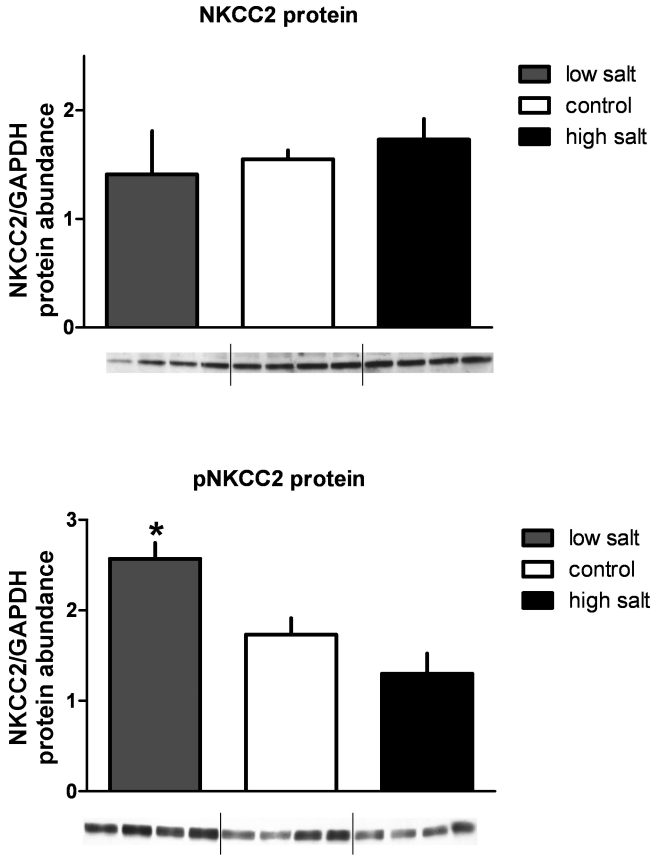

Fig. 3. NKCC2 protein and phospho-NKCC2 protein after modulation of the oral salt intake. Western blotting for NKCC2 (*A*) and pNKCC2 (*B*) was performed on kidney protein extracts from mice after 7 days on a high-salt [4% NaCl (wt/wt)], standard [0.4% NaCl (wt/wt)], and a low-salt diet [0.02% NaCl (wt/wt)]. *$P < 0.05$ vs. control. Representative immunoblots for NKCC2 and pNKCC2 are shown under bar graphs.

the renin angiotensin system, and angiotensin receptors have been shown to be expressed along the TAL. Therefore, we next addressed the role of angiotensin II in the regulation of the splicing process of the NKCC2 pre-mRNA. For this purpose, mice were chronically infused with angiotensin II via osmotic minipumps (2 mg·kg^{-1}·day^{-1}). Angiotensin II infusion resulted in an increase in arterial blood pressure averaging 165 ± 5 mmHg compared with 112 ± 4 mmHg in vehicle-infused controls ($P < 0.01$). After 7 days of angiotensin II infusion, the total NKCC2 mRNA expression slightly increased without reaching levels of significance in the OMOS and cortex. There was a marked shift in the expression of NKCC2 isoforms in the cortex similarly to that during the salt-restricted diet. The NKCC2B levels increased and the NKCC2A abundance decreased relative to those in vehicle-infused mice (Fig. 5).

In view of the modulation of NKCC2 expression and splicing during angiotensin II infusion, we next determined the type of receptor that mediated the effect of angiotensin II. Mice received the AT_1 receptor antagonist losartan (30 mg·kg^{-1}·day^{-1}) and the AT_2 receptor antagonist PD123319 (10 mg·kg^{-1}·day^{-1}) for 7 days, after which the NKCC2 isoform expression was determined. Losartan changed the NKCC2 isoform expression opposite to the change observed for the angiotensin II infusion, as shown in detail in Fig. 5. In contrast, PD123319 administration did not influence the absolute or relative expression levels of any NKCC2 isoform (not shown).

Table 1. *Summary of key physiological parameters determined during the in vivo experiments*

Parameters	Measurements
24-h Na^+ excretion, mmol·day^{-1}·30 g^{-1}	
High salt	11.5 ± 2.2*
Standard diet	2.2 ± 0.4
Low salt	0.30 ± 0.01*
Urine osmolarity, mosmol/kgH_2O	
Furosemide	355 ± 100*
Control	1,625 ± 188
Water restriction	3,320 ± 405*
DDAVP	2,650 ± 320*
Sugar water	360 ± 100*
Blood pressure (tail cuff measurement), mmHg	
Angiotensin II infusion	165 ± 5*
Control	112 ± 4
Losartan	105 ± 5
PD123319	110 ± 8
Losartan/low salt	94 ± 6*

Values are means ± SE. DDAVP, 1-desamino-8-D-arginine-vasopressin. *$P < .05$ vs. control.

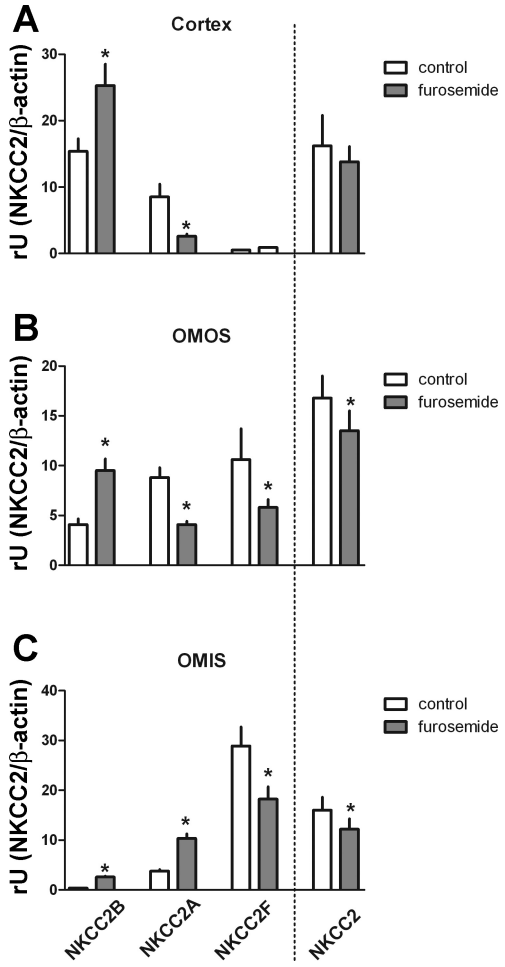

Fig. 4. Inhibition of NKCC2 transport activity by furosemide modulates NKCC2 isoform abundance. Furosemide (10 mg·kg^{-1}·day^{-1}) was administered via osmotic minipumps and NKCC2 isoform expression was determined after 7 days: cortex (*A*), OMOS (*B*), and OMIS (*C*). *$P < 0.05$ vs. vehicle.

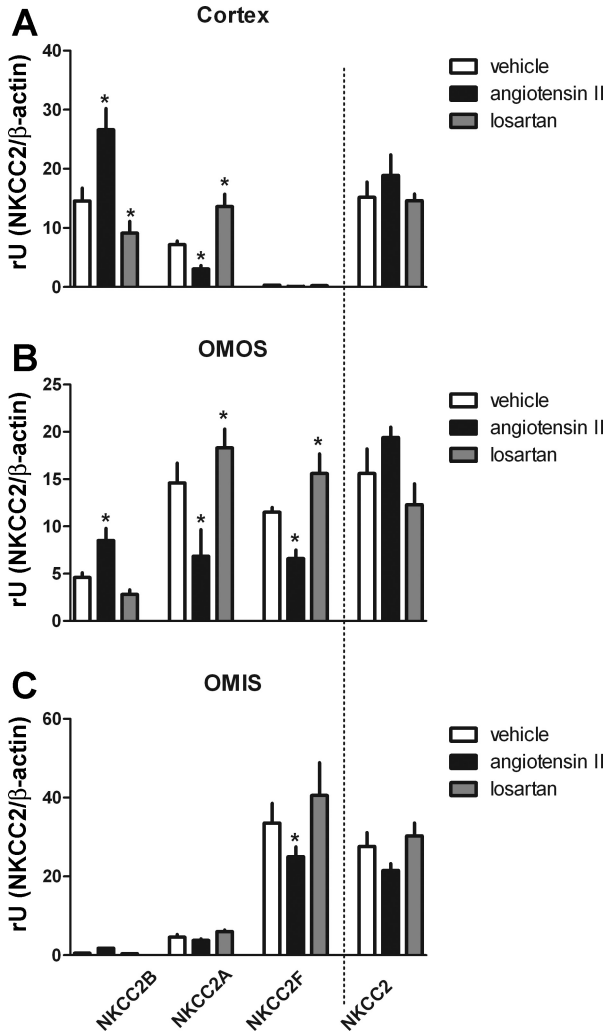

Fig. 5. AT_1 receptor-dependent effects of the renin angiotensin system influence NKCC2 isoform abundance. mRNA expression of NKCC2 isoforms after chronic infusion of angiotensin II (2 mg·kg^{-1}·day^{-1}) and the AT_1 antagonist losartan (30 mg·kg^{-1}·day^{-1}): cortex (*A*), OMOS (*B*), and OMIS (*C*). *$P <$ 0.05 vs. vehicle.

To further establish a possible cause-effect correlation for the regulation of the NKCC2 differential splicing during a salt-restricted diet by angiotensin II, we next combined a low-salt diet with the AT_1 receptor antagonist losartan. Again, during a low-salt diet, the expression pattern of the NKCC2 isoforms shifted from NKCC2A to NKCC2B in the cortex and OMOS, as shown in Fig. 6. When a low-salt diet was combined with the AT_1 antagonist losartan, the magnitude of the changes in the expression levels of the single isoforms was markedly reduced, indicating a partial AT_1 receptor-dependent effect (Fig. 6).

In Vitro Analysis of the Effects of Furosemide and Angiotensin II on NKCC2 Differential Splicing

To assess the regulation of the differential splicing of NKCC2 under controlled in vitro conditions, kidney slices were incubated in a perfusion chamber system (48 h). The baseline expression of the NKCC2 isoforms in cultured kidney slices differed from the in vivo situation, with NKCC2A being the dominant isoform, as summarized in Fig. 7. Furosemide (100 μM) reduced the abundance of the A and F isoforms and increased the expression of the B isoform, similar to the regulation that was observed in vivo (Fig. 7*A*). Angiotensin II (10 nM) increased the expression of all NKCC2 isoforms without altering the distribution pattern of the single isoforms (Fig. 7*B*). The effect of angiotensin II was blocked in the presence of losartan (100 nM), whereas the AT_2 antagonist PD123319 (100 nM) did not influence the NKCC2 isoform expression during incubation with angiotensin II ($n = 9$ slices for each condition; Fig. 7*B*).

Influence of Water Restriction and Water Loading on NKCC2 Differential Splicing

Water restriction for 48 h resulted in an induction of all NKCC2 isoforms independent of their zonal localization. Thus, compared with mice with free access to water, water restriction enhanced the total NKCC2 abundance by 85, 118, and 79% in the cortex, OMOS, and OMIS, respectively (Fig. 8). For the single isoforms, water restriction induced NKCC2B levels in the cortex and OMOS. As in the control animals, the NKCC2B abundance in the OMIS was low. Similarly, the NKCC2A and NKCC2F abundance increased in all kidney zones, with the absolute levels of NKCC2F in the cortex being close to the

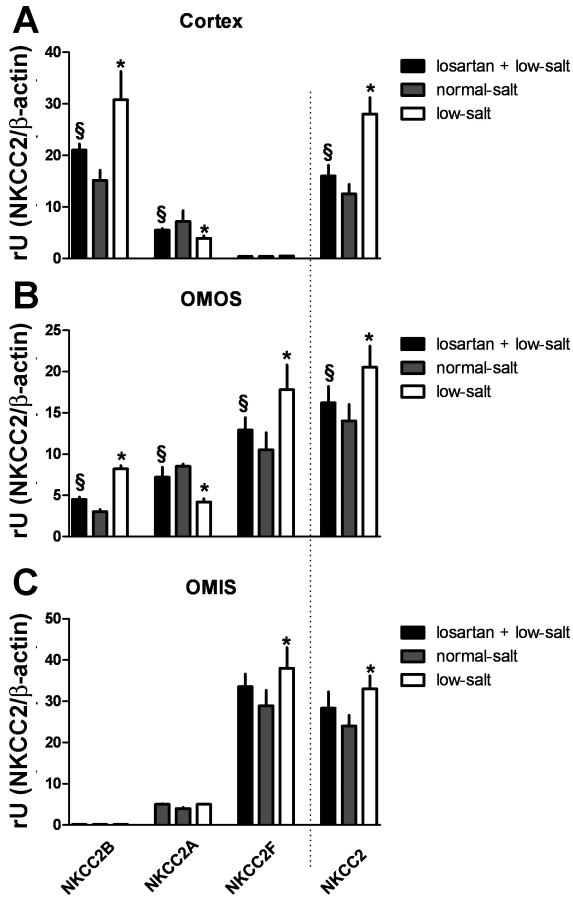

Fig. 6. AT_1 receptor antagonism partially reverses the effects of a low-salt diet on NKCC2 isoform abundance. Losartan (30 mg·kg^{-1}·day^{-1}) was administered in the drinking water in combination with a low-salt diet [0.02% NaCl (wt/wt)]: cortex (*A*), OMOS (*B*), and OMIS (*C*). *$P < 0.05$ vs. control. §$P <$ 0.05 vs. low-salt diet.

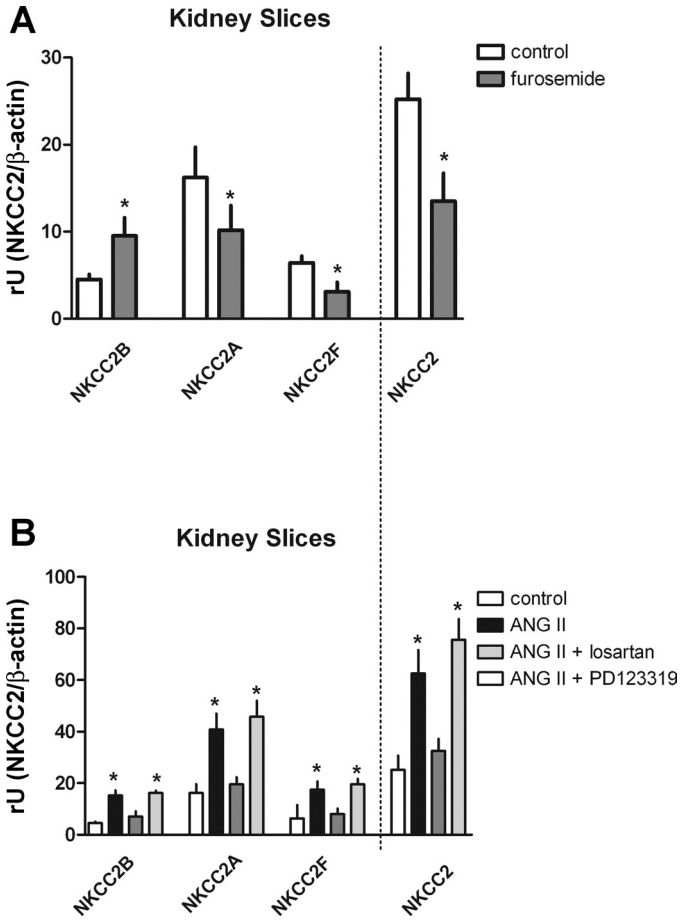

Fig. 7. NKCC2 isoform expression in vitro. *A*: furosemide modulates NKCC2 expression in cultured kidney slices. mRNA expression of NKCC2 isoforms after addition of furosemide (100 μM) to the perfusion medium. *B*: mRNA expression of NKCC2 isoforms after superfusion of kidney slices with angiotensin II (10 nM), angiotensin II (10 nM) + losartan (100 nM), and angiotensin II (10 nM) + PD123319 (100 nM). *$P < 0.05$ vs. vehicle.

detection limit. Water restriction was accompanied by a marked increase in the spot urine osmolarity from 1,625 ± 188 to 3,320 ± 405 mosmol/kgH_2O ($n = 8$; Table 1). Therefore, we next considered interstitial osmolarity as a modulator of NKCC2 differential splicing and/or overall NKCC2 mRNA expression. To decrease the urine osmolarity below the ambient osmolarity, mice were offered sugar water (8% sucrose) in addition to tap water. Mice preferred the sugar solution over the tap water and increased their daily water intake markedly, resulting in a drop in ambient osmolarity to 360 ± 100 mosmol/kgH_2O. In contrast to restraining mice from water access, the water loading suppressed NKCC2 mRNA levels but again did not alter the distribution pattern of the NKCC2 isoforms, as shown in Fig. 8.

Because the abundance of all the NKCC2 isoforms increased and decreased in parallel during water restriction and water loading, we used these experimental maneuvers to assess if changes in the mRNA abundances of the NKCC2 isoforms result in altered NKCC2 protein levels. The NKCC2 protein normalized to the GAPDH abundance was 0.56 ± 0.04, 0.72 ± 0.05, and 1.32 ± 0.09 rU for water loading, control, and water restriction, respectively ($n = 4$; $P < 0.01$ for water restriction vs. control and $P < 0.05$ for water loading vs. control). Similarly, the pNKCC2 abundance averaged 1.94 ± 0.24, 2.18 ± 0.22, and 2.85 ± 0.11 rU for water loading, control, and water restriction, respectively ($n = 4$; $P < 0.05$ for water restriction vs. control; Fig. 9).

In view of the regulation of NKCC2 isoform expression by water restriction we next determined the effect of vasopressin on the differential splicing of NKCC2. Mice were chronically infused with the V2 receptor agonist DDAVP (2 $\mu g \cdot kg^{-1} \cdot day^{-1}$), and the NKCC2 isoform levels were determined after 7 days. Infusion of DDAVP increased the ambient urine osmolarity to 2,460 ± 320 mosmol/kgH_2O, which contrasted with the 1,560 ± 188 mosmol/kgH_2O in vehicle-infused controls ($n = 6$; $P = 0.002$). As shown in Fig. 10, in contrast to water restriction, DDAVP infusion did not alter the abundance of total NKCC2 mRNA. Similarly, the expression levels of the different isoforms of the DDAVP-infused mice were indistinguishable from that of the controls.

DISCUSSION

Differential splicing is a widely observed phenomenon and contributes to the functional diversity of proteins (17). In the

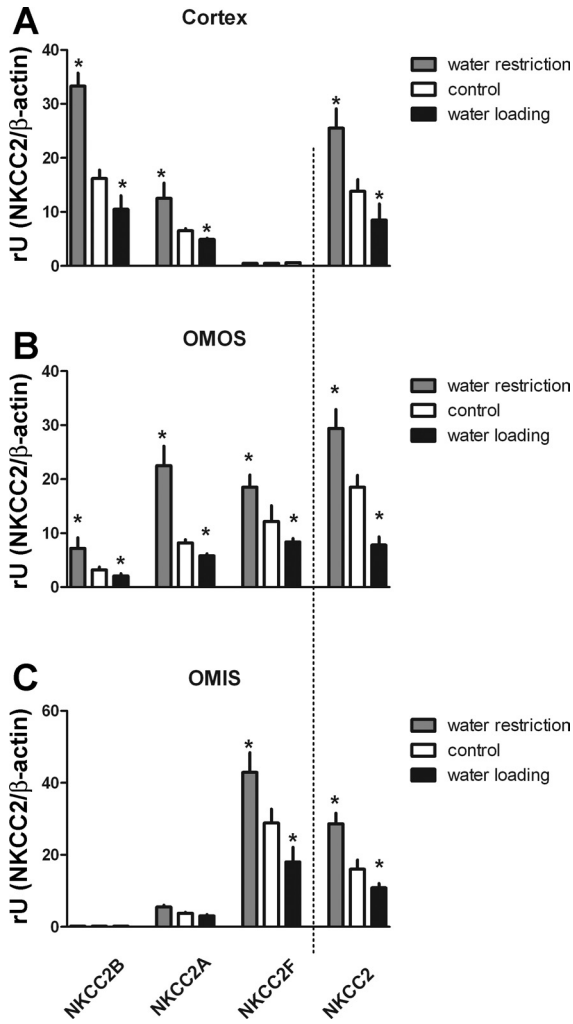

Fig. 8. Influence of water intake on NKCC2 isoform expression. mRNA expression of NKCC2 isoforms after water restriction (48 h) and water loading (8% sucrose solution in addition to tap water) and in controls (free access to tap water): cortex (*A*), OMOS (*B*), and OMIS (*C*). *$P < 0.05$ vs. vehicle.

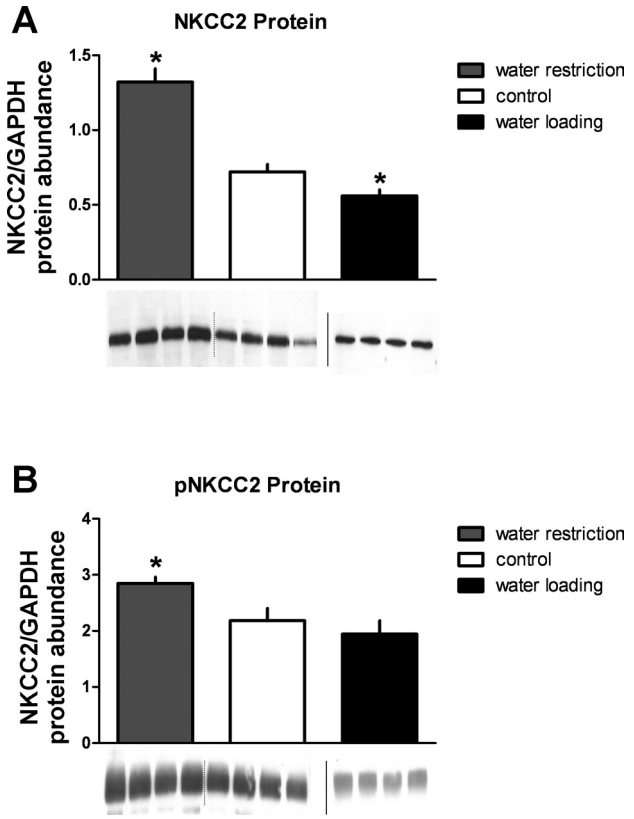

Fig. 9. Western blotting for NKCC2 (*A*) and pNKCC2 (*B*). NKCC2 and pNKCC2 protein abundance after water restriction (48 h), after water loading (8% sucrose solution in addition to tap water), and in controls (free access to tap water). *$P < 0.05$ vs. control. Representative immunoblots are shown under bar graphs.

present study we addressed the hypothesis that the differential splicing of the renal NKCC2 is influenced by external stimuli, and, consequently, may contribute to adaptations of TAL salt retrieval and macula densa salt sensing. For NKCC2, the three main splice isoforms differ substantially in their salt transport capacity and ion affinity. Thus, in rodents, the transport capacity decreases, and the ion affinity increases in the following order: NKCC2F > NKCC2A > NKCC2B (10, 29). The functional diversity of the isoforms is paralleled by a respective gradient of their expressions along the TAL. NKCC2F is the dominant isoform in the medullary TAL (high tubular NaCl concentrations), and NKCC2B expression levels are highest in the most downstream portions of the TAL (low tubular NaCl concentrations).

The key finding of this study was that the NKCC2 differential splicing was influenced by the dietary salt intake such that salt restriction induced a marked shift of the abundance of the single NKCC2 isoforms. Thus, in the renal cortex, NKCC2B was upregulated and NKCC2A was downregulated; similar changes occurred to a lesser extent in the OMOS. An inverse regulation of the NKCC2 isoform expression was found during a high-salt diet. Thus the differential splicing of NKCC2 is apparently a regulated process and may represent an adaptation of the TAL to salt reabsorptive needs. According to this assumption, the ion affinity and transport capacity of a particular TAL cell would change if a given amount of NKCC2 pre-mRNA is preferentially spliced to form the high-affinity B isoform of the cotransporter at the expense of the lower-affinity A isoform. This change may be functionally relevant, particularly in the most downstream portion of the TAL, where salt concentrations are low. Thus, the concentration of Cl, the transport-limiting ion, in the distal TAL decreases to the 35-mM concentration range (34). This value is close to the K_m for Cl for the A isoform, which was determined to be ~22 mM in the mouse, in contrast to 12 mM for the high-affinity B isoform (29).

In terms of the regulation of NKCC2A by the dietary salt intake, these results, at first glance, may appear to be contradictory to a recent study showing that NKCC2A in the renal medulla is induced in mice when given a 1% NaCl solution as drinking fluid (13). This maneuver, however, is not comparable to our regimen of salt-enriched food in combination with tap water, because it excludes osmoregulation by changes in fluid intake. Consequently, during volume loading with 1% NaCl solution, the renin angiotensin-system is massively suppressed (4), and this may account for increased NKCC2A expression, as discussed later.

Changes in dietary salt intake did not alter the net NKCC2 protein expression. We suggest that this finding reflects the

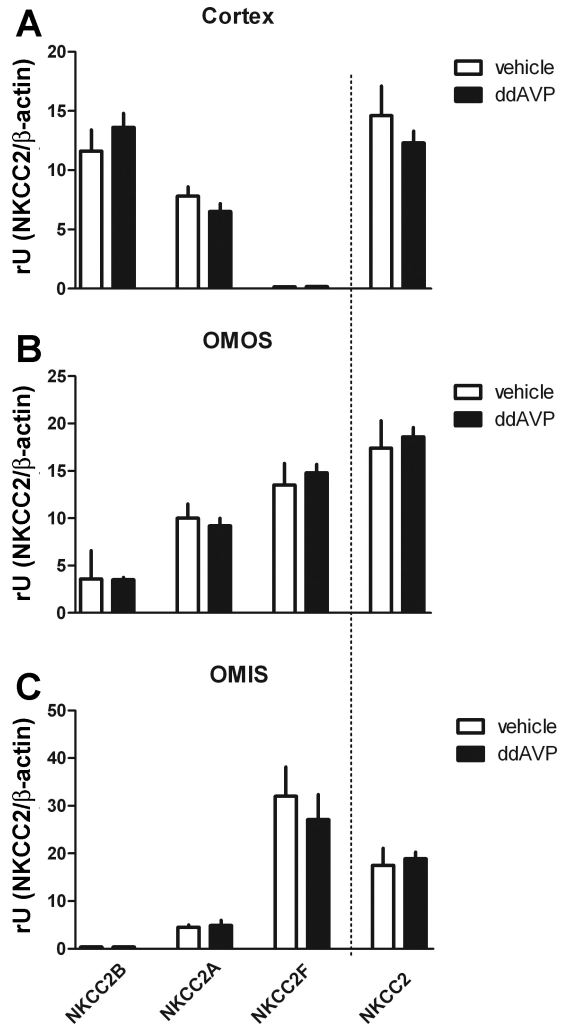

Fig. 10. Effect of DDAVP on NKCC2 isoform expression. mRNA expression of NKCC2 isoforms after infusion of DDAVP (2 $\mu g \cdot kg^{-1} \cdot day^{-1}$, 7 days) or vehicle: cortex (*A*), OMOS (*B*), and OMIS (*C*).

partly opposite regulation of the single mRNA isoforms, which would be expected to reduce net changes in the overall NKCC2 protein abundance. For an adaptation of the TAL to reduced salt intake, changes in the relative contribution of the single NKCC2 isoforms to overall NKCC2 abundance apparently are more relevant than the absolute level of the cotransporter. These data are consistent with a study in rats showing that the net protein expression of NKCC2 after 10 days of salt restriction was unchanged when compared with salt-repleted animals (21). Similar, a high-salt diet was shown not to modulate total NKCC2 abundance in the rat kidney (41). Conversely to total NKCC2 protein abundance, the phosphorylation status of NKCC2 increased when animals received a salt-restricted diet, suggesting posttranslational modifications of the cotransporter function (2, 6, 7, 18, 31).

The shift of the isoform-specific mRNA abundance from NKCC2A to NKCC2B during dietary salt restriction was largely recapitulated during administration of the loop diuretic furosemide. Thus NKCC2 transport activity appears to act as a sensor of the tubular NaCl concentration, which in turn influences differential splicing of the NKCC2 pre-mRNAs. These data are congruent with a recent report demonstrating increased NKCC2A and decreased NKCC2F expression in the total mouse kidney after 7 days of furosemide treatment (1). Furosemide also reduced the NKCC2F expression in the OMIS, the segment in which NKCC2F is the dominant isoform by far. Apparently, when NKCC2 transport activity in the presence of furosemide is low or absent, the NKCC2 isoform expression pattern of the OMIS changes to an expression pattern that more resembles the baseline expression pattern of the OMOS and the cortex. Consistent with this concept, downregulation of NKCC2F in the OMIS by furosemide was accompanied by increased levels of the B and A isoforms, whose baseline expression in the OMIS were low. Under normal conditions, there is a gradient of the NaCl concentration along the TAL, with chloride concentrations in the most distal portions of the TAL (in the area of the macula densa segment) dropping to $<$35 mM (34). Consequently, the NKCC2F expression level in the cortical TAL under baseline conditions was low, qualitatively similar to that in the OMIS during furosemide treatment. The cellular mechanism of this regulation of the differential splicing was not determined experimentally, but we speculate that intracellular ion concentrations may influence the splicing machinery. In this context, intracellular Cl^- has been shown to inversely influence NKCC2 transport activity, although this change was related to the protein levels (11, 32). Commensurate with this assumption, cultured kidney slices showed an isoform expression pattern with reduced NKCC2F but increased NKCC2A and NKCC2B isoforms, relative to those in the in vivo conditions. Thus, when compared with the tubular concentrations in the OMIS in vivo, the Cl concentration in the culture medium was low ($\sim$80 mM), leading to a preferential expression of the B isoform. The reduced NKCC2F and NKCC2A expression in vitro was further diminished in the presence of furosemide, recapitulating the in vivo results. Furosemide, however, may not have penetrated all the tissue of the kidney slices, which would quantitatively reduce net changes in isoform expression.

Furthermore, in NKCC2A-deficient mice, NKCC2B was upregulated in the renal cortex and the OMOS (27). The cells of the cortical TAL of the mouse express NKCC2B and NKCC2A (10, 26), and the specific genetic inactivation of NKCC2A presumably results in reduced overall NKCC2-dependent transport activity, as shown in micropuncture experiments (27). In this situation of compromised NaCl transport activity, NKCCA is upregulated, suggesting again that the differential splicing of the NKCC2 is modulated by the NKCC2 transport activity and, by inference, the intracellular ion composition.

Changes in dietary salt intake are accompanied by the inverse changes in the activity of the renin angiotensin system (4). In view of the results obtained during the high- and low-salt diets, we supposed that angiotensin II might be involved in regulating the differential splicing of NKCC2. Both the AT_1 and AT_2 receptors have been shown to be expressed in the TAL and to be relevant for TAL function (14, 15, 24, 30). Our experiments showed that chronic angiotensin II infusion led to a shift in the expression of NKCC2 from the A isoform to the B isoform similar to that which occurred for dietary salt restriction, and this regulation was most obvious in the renal cortex. Furthermore, combining the AT_1 receptor antagonist losartan with a salt-restricted diet partially suppressed the regulation of the NKCC2 isoform expression during salt deprivation, suggesting that AT_1 receptor activation during the low-salt diet contributes to the regulation of the NKCC2 isoforms. At the whole organ level, angiotensin II has recently been shown to increase the total NKCC2 mRNA expression in the rat (19, 43). These in vivo data, however, differ from the situation in vitro, as determined during incubation of kidney slices in the presence of angiotensin II. In the cultured kidney slices, angiotensin II acting on the AT_1 receptor stimulated the expression of NKCC2 with no apparent isoform specificity, suggesting that angiotensin II in vivo affected the isoform expression indirectly rather than directly. Thus elevated angiotensin II concentrations have been shown to reduce the glomerular filtration rate and increase proximal tubular salt reabsorption, both of which would convert the TAL into a situation with reduced local salt concentration. An indirect, transport-dependent effect of angiotensin II was also suggested by the regulation of NKCC2F in the OMIS. Thus NKCC2F in the OMIS was downregulated during angiotensin II infusion. This downregulation was similar to that during furosemide, albeit to a much lower extent.

NKCC2 transport activity facilitates the bulk of TAL transepithelial salt transport. In addition, NKCC2-dependent salt transport accounts for macula densa salt sensing and triggers the signaling cascades within the juxtaglomerular apparatus. Thus, macula densa salt transport by NKCC2 modulates renin secretion from granulated juxtaglomerular cells of the afferent arteriole and influences the tone of the afferent arteriole to control the single nephron GFR (TGF). Macula densa cells express the B and A isoforms of NKCC2. Studies in mice with specific inactivation of NKCC2B or NKCC2A also suggested that both isoforms cooperate in macula densa salt sensing, facilitating the detection of changes in tubular Cl over a wide range of concentrations (26, 27). Thus, in NKCC2B-deficient mice, the TGF response curves were right-shifted compared with those in wild-type mice, whereas the TGF curve was left shifted in NKCC2A-deficient animals, and the maximum response magnitude was reduced. Theses findings suggest that NKCC2B primarily accounts for salt sensing in the low concentration range, whereas NKCC2A mediates salt sensing in

the high concentration range, when NKCC2B transport activity is fully saturated. During prolonged exposure to deviated tubular salt concentration, TGF responsiveness is restored by resetting mechanisms that change the operating point of the TGF feedback loop (36, 37). The shift from the low-affinity A isoform to the high-affinity B isoform in the renal cortex during chronic salt deprivation may contribute to this resetting of the TGF, rendering the macula densa cells more sensitive in the low Cl concentration range.

In contrast to the changes in oral salt intake, which appeared to specifically regulate NKCC2 differential splicing in a site-specific manner, the changes in water consumption, such as water restriction and water loading, had a general impact on the NKCC2 mRNA transcription and/or mRNA stability, without influencing the relative abundance of the single isoforms. Thus the NKCC2 mRNA expression was altered by water intake, with water restriction stimulating and water loading suppressing the expression of all isoforms. This regulation at the mRNA level was paralleled by corresponding changes in the NKCC2 protein abundance and in the protein phosphorylation status. These data are consistent with recent studies in male Fisher 344 x Brown Norway and in Sprague-Dawley rats, reporting increased protein expression of NKCC2 after water restriction (6, 39).

Water restriction results in markedly elevated vasopressin levels (25). The regulation of the NKCC2 mRNA during water restriction appeared to be independent of the V2 vasopressin receptors because infusion of the V2 agonist DDAVP did not alter the NKCC2 mRNA expression, indicating a V2-independent effect. A more direct assessment of the cause-effect of vasopressin on the differential splicing of NKCC2 during water restriction, such as the combination of water restriction and the application of a V2 receptor antagonist, is problematic because V2-mediated concentrating ability during water restriction is crucial for the survival of the animals during this condition. Similar results were recently obtained for rats. Again, water loading led to decreased expression levels of the NKCC2 A and F isoform (1). In contrast to NKCC2 mRNA expression, vasopressin has been shown to increase NKCC2 protein abundance and the protein phosphorylation status, resulting in augmented membrane trafficking (2, 6, 9, 18, 31).

As a limitation to this study, the expression of the NKCC2 isoforms was determined at the mRNA levels. Presumably due to the high similarity between the NKCC2 isoforms, all our attempts to generate isoform-specific antibodies were unsuccessful. When using kidneys from NKCC2B -and NKCC2A-deficient mice (26, 27), several different antibodies raised against NKCC2B and NKCC2A produced similar signals like what was seen in wild-type tissues (immunohistochemistry and Western blotting), suggesting that there was unspecific binding and cross-reactivity of the antibodies to the remaining isoforms. Nevertheless, when the expression levels of all isoforms changed in the same way, such as during water restriction, the mRNA and total protein levels of NKCC2 changed in parallel, suggesting that the amount of mRNA determines the expression level of the NKCC2 protein.

In summary, differential splicing of NKCC2 pre-mRNA is regulated by dietary salt intake and may therefore participate in long-term adaptive processes of the TAL. Our data suggest that the NKCC2 transport activity and, by inference, intracellular ion composition participate in the modulation of the splicing process. Although multiple additional mechanisms may impinge on the splicing process, our data suggest a common regulatory pattern characterized by a preferential formation of the higher affinity isoforms in situations of reduced NKCC2 transport activity. This general pattern appears to be modulated by hormones, such as angiotensin II.

GRANTS

This study was supported by a grant from the Deutsche Forschungsgemeinschaft (SFB699/A4).

DISCLOSURES

No conflicts of interest, financial or otherwise, are declared by the author(s).

AUTHOR CONTRIBUTIONS

Author contributions: I.M.S., A.R., V.K., W.W.M., M.O., and H.C. performed experiments; I.M.S., A.R., V.K., W.W.M., M.O., and H.C. analyzed data; I.M.S., A.R., and H.C. interpreted results of experiments; I.M.S. and H.C. edited and revised manuscript; I.M.S., A.R., V.K., W.W.M., M.O., and H.C. approved final version of manuscript; H.C. conception and design of research; H.C. prepared figures; H.C. drafted manuscript.

REFERENCES

1. **Brunet GM, Gagnon E, Simard CF, Daigle ND, Caron L, Noel M, Lefoll MH, Bergeron MJ, Isenring P.** Novel insights regarding the operational characteristics and teleological purpose of the renal Na^+-K^+-Cl2 cotransporter (NKCC2s) splice variants. *J Gen Physiol* 126: 325–337, 2005.
2. **Caceres PS, Ares GR, Ortiz PA.** cAMP stimulates apical exocytosis of the renal Na(+)-K(+)-2Cl(-) cotransporter NKCC2 in the thick ascending limb: role of protein kinase A. *J Biol Chem* 284: 24965–24971, 2009.
3. **Carota I, Theilig F, Oppermann M, Kongsuphol P, Rosenauer A, Schreiber R, Jensen BL, Walter S, Kunzelmann K, Castrop H.** Localization and functional characterization of the human NKCC2 isoforms. *Acta Physiol (Oxf)* 199: 327–338, 2010.
4. **Castrop H, Hocherl K, Kurtz A, Schweda F, Todorov V, Wagner C.** Physiology of kidney renin. *Physiol Rev* 90: 607–673, 2010.
5. **Castrop H, Schnermann J.** Isoforms of renal Na-K-2Cl cotransporter NKCC2: expression and functional significance. *Am J Physiol Renal Physiol* 295: F859–F866, 2008.
6. **Ecelbarger CA, Kim GH, Wade JB, Knepper MA.** Regulation of the abundance of renal sodium transporters and channels by vasopressin. *Exp Neurol* 171: 227–234, 2001.
7. **Flemmer AW, Gimenez I, Dowd BF, Darman RB, Forbush B.** Activation of the Na-K-Cl cotransporter NKCC1 detected with a phospho-specific antibody. *J Biol Chem* 277: 37551–37558, 2002.
8. **Gamba G, Miyanoshita A, Lombardi M, Lytton J, Lee WS, Hediger MA, Hebert SC.** Molecular cloning, primary structure, and characterization of two members of the mammalian electroneutral sodium-(potassium)-chloride cotransporter family expressed in kidney. *J Biol Chem* 269: 17713–17722, 1994.
9. **Gimenez I, Forbush B.** Short-term stimulation of the renal Na-K-Cl cotransporter (NKCC2) by vasopressin involves phosphorylation and membrane translocation of the protein. *J Biol Chem* 278: 26946–26951, 2003.
10. **Gimenez I, Isenring P, Forbush B.** Spatially distributed alternative splice variants of the renal Na-K-Cl cotransporter exhibit dramatically different affinities for the transported ions. *J Biol Chem* 277: 8767–8770, 2002.
11. **Haas M, Forbush B 3rd.** The Na-K-Cl cotransporters. *J Bioenerg Biomembr* 30: 161–172, 1998.
12. **Haas M, McManus TJ.** Bumetanide inhibits (Na^+-K^+-2Cl) cotransport at a chloride site. *Am J Physiol Cell Physiol* 245: C235–C240, 1983.
13. **Hao S, Bellner L, Ferreri NR.** NKCC2A and NFAT5 regulate renal TNF production induced by hypertonic NaCl intake. *Am J Physiol Renal Physiol* 304: F533–F542, 2013.
14. **Herrera M, Garvin JL.** Angiotensin II stimulates thick ascending limb NO production via AT(2) receptors and Akt1-dependent nitric-oxide synthase 3 (NOS3) activation. *J Biol Chem* 285: 14932–14940.
15. **Herrera M, Silva GB, Garvin JL.** Angiotensin II stimulates thick ascending limb superoxide production via protein kinase C(alpha)-dependent NADPH oxidase activation. *J Biol Chem* 285: 21323–21328.

16. **Igarashi P, Vanden Heuvel GB, Payne JA, Forbush B, 3rd.** Cloning, embryonic expression, and alternative splicing of a murine kidney-specific Na-K-Cl cotransporter. *Am J Physiol Renal Fluid Electrolyte Physiol* 269: F405–F418, 1995.
17. **Kan Z, Rouchka EC, Gish WR, States DJ.** Gene structure prediction and alternative splicing analysis using genomically aligned ESTs. *Genome Res* 11: 889–900, 2001.
18. **Knepper MA, Kim GH, Fernandez-Llama P, Ecelbarger CA.** Regulation of thick ascending limb transport by vasopressin. *J Am Soc Nephrol* 10: 628–634, 1999.
19. **Kwon TH, Nielsen J, Kim YH, Knepper MA, Frokiaer J, Nielsen S.** Regulation of sodium transporters in the thick ascending limb of rat kidney: response to angiotensin II. *Am J Physiol Renal Physiol* 285: F152–F165, 2003.
20. **Lapointe JY, Bell PD, Cardinal J.** Direct evidence for apical Na^+-$2Cl^-$-K^+ cotransport in macula densa cells. *Am J Physiol Renal Fluid Electrolyte Physiol* 258: F1466–F1469, 1990.
21. **Masilamani S, Wang X, Kim GH, Brooks H, Nielsen J, Nielsen S, Nakamura K, Stokes JB, Knepper MA.** Time course of renal Na-K-ATPase, NHE3, NKCC2, NCC, and ENaC abundance changes with dietary NaCl restriction. *Am J Physiol Renal Physiol* 283: F648–F657, 2002.
22. **Mederle K, Mutig K, Paliege A, Carota I, Bachmann S, Castrop H, Oppermann M.** Loss of WNK3 is compensated for by the WNK1/SPAK axis in the kidney of the mouse. *Am J Physiol Renal Physiol* 304: F1198–F1209, 2013.
23. **Minuth WW, Strehl R, Schumacher K, de Vries U.** Long term culture of epithelia in a continuous fluid gradient for biomaterial testing and tissue engineering. *J Biomater Sci Polym Ed* 12: 353–365, 2001.
24. **Miyata N, Park F, Li XF, Cowley AW Jr.** Distribution of angiotensin AT_1 and AT_2 receptor subtypes in the rat kidney. *Am J Physiol Renal Physiol* 277: F437–F446, 1999.
25. **Morton JJ, Padfield PL, Forsling ML.** A radioimmunoassay for plasma arginine-vasopressin in man and dog: application to physiological and pathological states. *J Endocrinol* 65: 411–424, 1975.
26. **Oppermann M, Mizel D, Huang G, Li C, Deng C, Theilig F, Bachmann S, Briggs J, Schnermann J, Castrop H.** Macula densa control of renin secretion and preglomerular resistance in mice with selective deletion of the B isoform of the Na,K,2Cl co-transporter. *J Am Soc Nephrol* 17: 2143–2152, 2006.
27. **Oppermann M, Mizel D, Kim SM, Chen L, Faulhaber-Walter R, Huang Y, Li C, Deng C, Briggs J, Schnermann J, Castrop H.** Renal function in mice with targeted disruption of the A isoform of the Na-K-2Cl co-transporter. *J Am Soc Nephrol* 18: 440–448, 2007.
28. **Payne JA, Forbush B, 3rd.** Alternatively spliced isoforms of the putative renal Na-K-Cl cotransporter are differentially distributed within the rabbit kidney. *Proc Natl Acad Sci USA* 91: 4544–4548, 1994.
29. **Plata C, Meade P, Vazquez N, Hebert SC, Gamba G.** Functional properties of the apical Na^+-K^+-2Cl- cotransporter isoforms. *J Biol Chem* 277: 11004–11012, 2002.
30. **Poumarat JS, Houillier P, Rismondo C, Roques B, Lazar G, Paillard M, Blanchard A.** The luminal membrane of rat thick limb expresses AT1 receptor and aminopeptidase activities. *Kidney Int* 62: 434–445, 2002.
31. **Rieg T, Tang T, Uchida S, Hammond HK, Fenton RA, Vallon V.** Adenylyl cyclase 6 enhances NKCC2 expression and mediates vasopressin-induced phosphorylation of NKCC2 and NCC. *Am J Pathol* 182: 96–106, 2013.
32. **Russell JM.** Sodium-potassium-chloride cotransport. *Physiol Rev* 80: 211–276, 2000.
33. **Schlatter E, Salomonsson M, Persson AE, Greger R.** Macula densa cells sense luminal NaCl concentration via furosemide sensitive Na^+2Cl-K^+ cotransport. *Pflügers Arch* 414: 286–290, 1989.
34. **Schnermann J, Briggs J, Schubert G.** In situ studies of the distal convoluted tubule in the rat. I. Evidence for NaCl secretion. *Am J Physiol Renal Fluid Electrolyte Physiol* 243: F160–F166, 1982.
35. **Schumacher K, Strehl R, Kloth S, Tauc M, Minuth WW.** The influence of culture medi on embryonic renal collecting duct cell differentiation. In Vitro *Cell Dev Biol Anim* 35: 465–471, 1999.
36. **Thomson SC, Bachmann S, Bostanjoglo M, Ecelbarger CA, Peterson OW, Schwartz D, Bao D, Blantz RC.** Temporal adjustment of the juxtaglomerular apparatus during sustained inhibition of proximal reabsorption. *J Clin Invest* 104: 1149–1158, 1999.
37. **Thomson SC, Blantz RC, Vallon V.** Increased tubular flow induces resetting of tubuloglomerular feedback in euvolemic rats. *Am J Physiol Renal Fluid Electrolyte Physiol* 270: F461–F468, 1996.
38. **Thurau K, Schnermann J.** [The sodium concentration in the macula densa cells as a regulating factor for glomerular filtration (micropuncture experiments)]. *Klin Wochenschr* 43: 410–413, 1965.
39. **Tian Y, Riazi S, Khan O, Klein JD, Sugimura Y, Verbalis JG, Ecelbarger CA.** Renal ENaC subunit, Na-K-2Cl and Na-Cl cotransporter abundances in aged, water-restricted F344 x Brown Norway rats. *Kidney Int* 69: 304–312, 2006.
40. **Vargas-Poussou R, Feldmann D, Vollmer M, Konrad M, Kelly L, van den Heuvel LP, Tebourbi L, Brandis M, Karolyi L, Hebert SC, Lemmink HH, Deschenes G, Hildebrandt F, Seyberth HW, Guay-Woodford LM, Knoers NV, Antignac C.** Novel molecular variants of the Na-K-2Cl cotransporter gene are responsible for antenatal Bartter syndrome. *Am J Hum Genet* 62: 1332–1340, 1998.
41. **Yang LE, Sandberg MB, Can AD, Pihakaski-Maunsbach K, McDonough AA.** Effects of dietary salt on renal Na^+ transporter subcellular distribution, abundance, and phosphorylation status. *Am J Physiol Renal Physiol* 295: F1003–F1016, 2008.
42. **Yang T, Huang YG, Singh I, Schnermann J, Briggs JP.** Localization of bumetanide- and thiazide-sensitive Na-K-Cl cotransporters along the rat nephron. *Am J Physiol Renal Fluid Electrolyte Physiol* 271: F931–F939, 1996.
43. **Ye T, Liu ZQ, Sun CF, Zheng Y, Ma AQ, Fang Y.** Altered expression of renal bumetanide-sensitive sodium-potassium-2 chloride cotransporter and Cl- channel -K2 gene in angiotensin II-infused hypertensive rats. *Chin Med J (Engl)* 118: 1945–1951, 2005.